

BBAMEM 75004

Specific electroporabilization of leucocytes in a blood sample and application to large volumes of cells

S. Sixou and J. Teissié

Centre de Recherche de Biochimie et Génétique Cellulaires du CNRS, Toulouse (France)

(Received 19 April 1990)

Key words: Electroporabilization; Leucocyte; Erythrocyte; (Chinese hamster ovary cells)

Electroporabilization is obtained when the membrane potential difference reaches a critical threshold. This is performed by submitting cells to an external electric field pulse. The field modulates the endogenous potential difference in a cell-size-dependent way. Computer simulations predict that large cells would be specifically permeabilized in a mixture with smaller cells. This was examined on a mixture of Chinese hamster ovary (CHO) cells and erythrocytes. CHO cells were permeabilized to Trypan blue without any occurrence of haemolysis. A similar 'size' specificity was observed on blood samples. This agreement between prediction and experimental observation indicates that induction of electroporabilization is mainly under the control of the size of the target cell. Its physiology plays only a minor role, if any. Treating blood with 10 square wave pulses lasting 100 μ s of an intensity of 1.6 kV/cm induced the permeabilization of 70% of the leucocytes (polymorphs and monocytes) but did not affect erythrocytes. No washing of the sample was needed in a procedure in which cells were pulsed in the plasma. A flow electropulsing process allows the treatment of large blood volumes under conditions where cells are kept viable. These results show that electroporabilization could be used as an effective way to obtain immunocompatible drug vehicles.

Introduction

Electroporabilization of the cell membrane is an efficient tool to introduce non-permeant molecules such as dyes or drugs in the cell cytoplasm [1–7]. Because this technique is fast and simple, it is applicable for basic purposes as well as for biotechnology. Electrical parameters (field intensity, time duration, number of pulses) can be adapted to each cell type in order to keep pulsed cells viable. Electroporabilization, by giving access to the cytoplasm [8], allows the loading of viable cells with exogenous molecules. Such a loading appears as an elegant way to obtain drug vehicles. The pharmacological applications of electroporabilization have been first performed on red blood cells by electroloading ghosts [9] or erythrocytes [10,11] that might serve as intravenous drug vehicles which slowly release the drug into the circulation. Increasing antitumor drug activities by electroporabilization of cells has been observed,

suggesting that the uptake across the plasma membrane is a rate-limiting factor [3–5]. Electrotransformation of murine hematopoietic cells was obtained with genomic DNA [12]. This result opens interesting prospects for gene therapy. These studies are all indicative of the interesting medical potentialities of electroporabilization. An important prerequisite for efficient drug carriers is specificity. A huge amount of work tries to improve the drug efficiencies by increasing their uptake at the targeted site and by decreasing the side effects on other tissues and organs. Drugs must be slowly released to increase their plasma lifetime. Many systems have been developed (for reviews, see Refs. 13 and 14) such as liposomes [15,16], erythrocyte ghosts [17,18], synthetic and biological macromolecules [19–21], immunotoxins [22] and prodrugs [23,24]. The efficiency of these carriers requires them to be non-toxic, biodegradable and biocompatible [25].

'In vivo' experiments of electroloading or electrotransformation have studied the functional activities of pulsed cells and have shown that (i) electroloaded murine erythrocytes injected back into donor mice had a lifetime similar to that of normal cells [11], (ii) no significant loss in metabolic and functional potential was observed for electroporabilized human blood platelets [26], (iii) murine hematopoietic cells electro-

Abbreviations: CHO cells, Chinese hamster ovary cells; PB, pulsing buffer.

Correspondence: J. Teissié, Centre de Recherche de Biochimie et Génétique Cellulaires du CNRS, 118 route de Narbonne, 31062 Toulouse cedex, France.

transformed and injected into lethally irradiated mice expressed the gene in hematopoietic tissues 14 days after pulsing [12].

These studies demonstrated the integrity and biocompatibility of pulsed cells and suggest that pulsed blood cells can be used as drug vehicles.

White blood cells are fully adapted to the use as 'antibiotic carrier' because they have a functional specificity (fast accumulation in infectious sites [27]) and are also immunocompatible. Nevertheless, electroporation of isolated leucocytes has only been used for lymphocyte transformation experiments [12,28,29]. The present study establishes that electroloading of leucocytes can be made in a blood sample without alteration of erythrocytes and that the leucocyte viability is maintained. Furthermore, a flow system was used to treat large cell volumes.

Materials and Methods

Cell preparation

Culture of chinese hamster ovary (CHO) cells. CHO cells (WTT clone) were grown in suspension by using a spinner flask (500 ml) driven by a magnetic stirrer (400 rpm). The culture temperature was set at 37°C. The culture medium was Eagle's minimum essential medium (MEM 0111, Eurobio, France) supplemented with 6% new born calf serum (Boehringer, F.R.G.), penicillin (100 UI/ml), streptomycin (100 µg/ml) and L-glutamine (0.58 mg/ml). The cell density was maintained between $4 \cdot 10^5$ and $1.5 \cdot 10^6$ cells per ml (exponential growth phase) by daily dilution in the culture medium.

Blood cells. Blood samples were kindly provided by Dr Tarbes (CTS Rangueil, Toulouse, France). Erythrocytes were obtained by centrifuging blood samples ($2000 \times g$, 5 min, room temperature) and removing supernatant. Leucocytes were used as 'leucocyte concentrates': after elimination of most of the erythrocytes by centrifugation of blood samples ($1100 \times g$, 30 min), a 1/100 leucocyte and erythrocyte mixture is obtained.

Permeabilization

Experiments were performed at 21°C in an air-conditioned room, in the following low ionic content saline buffer: 125 mM sucrose, 69 mM KCl, 1 mM MgCl₂ in 10 mM phosphate buffer (pH 7.4). This 'pulsing buffer' (PB) was added after eliminating culture medium or plasma by centrifugation ($100 \times g$, 4 min or $2000 \times g$, 5 min, respectively, at room temperature). Cells were washed twice in PB. For experiments on blood samples, cells were directly pulsed in plasma.

Electroporation was carried out using a CNRS electropulser (Jouan, France) able to deliver square-wave pulses which parameters (voltage, pulse duration, number and frequency of pulses) are all independently adjustable. Pulses were monitored using a 5

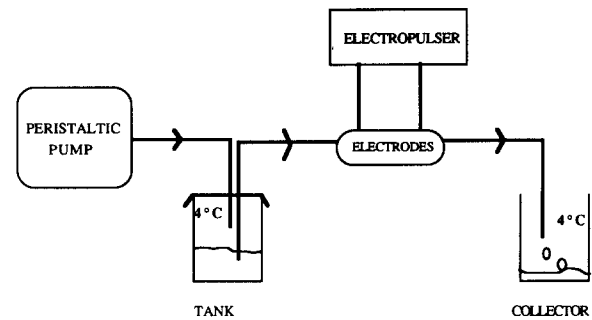


Fig. 1. Continuous flow electropulser. The flow was generated by the air pressure created by the pump. Cell flow was submitted to controlled electrical pulses between the electrodes. Sterility was maintained by working under a laminar flow hood.

MHz oscilloscope (Enertec, France). For the 'batch experiments', the system was as follows: electrodes are parallel and flat with an anode-cathode distance of 4.3 mm. 250 µl of cell suspension were treated by bringing electrodes into contact with a culture dish in order to build an open chamber. The gap between the electrodes was then filled with the cell suspension and repetitive pulses were applied (10 pulses lasting 100 µs with a frequency of 1 Hz and various field intensities). Control cells were treated in a similar way except that no pulse was applied.

A flow system [30,31], described in fig. 1 was used: due to the pressure created by a peristaltic pump (Gilson, France), the cells flow between two parallel stainless-steel electrodes, 4 mm apart, which are the walls of a Plexiglass chamber containing 128 µl. The electropulser delivers electrical pulses with a frequency (up to 10 Hz) chosen as a function of the flow rate in such a way that successive pulses (duration 100 µs) are applied on each cell when it is present between the electrodes. If the frequency of pulses is F , then the flow f (ml/min) is obtained from the relationship:

$$f = (F \times 60 \times v) / n$$

where v is the volume of the pulsing chamber and n the number of applied pulses on a cell. Sterility of the flow system was obtained by washing the system with a flow of bleach for 20 min and then rinsing with sterile PB. The complete system was put in a laminar flow hood (ESI, France).

Determination of the permeabilization

CHO cells and leucocytes. Electroporation was quantitated by penetration of Ca²⁺ leading to cell lysis. Pulsed cells were mixed with PB containing 3 mM CaCl₂ and 1% (w/v) Trypan blue (Sigma, U.S.A.), incubated during 10 min and the number of blue-stained cells was counted in Ref. 32.

Erythrocytes. In case of erythrocytes, electroporation leads to a leakage of ions which in turn causes

the haemolysis of the erythrocytes [10,11]. The haemoglobin leakage was quantified by incubating aliquots of pulsed samples (about 10^8 erythrocytes in 50 μ l) in 2 ml of PB during 2 h at 4°C. The samples were then spun down ($2500 \times g$, 5 min, room temperature) and the absorbance at 413 nm of the supernatant was recorded. 100% haemolysis was obtained from a hypotonic shocked sample using pure water [11].

The size histograms were obtained by use of a video system. Cells were videomonitoried with an inverted phase microscope (Diavert, Leitz, F.R.G.) coupled to a camera (JVC, Japan). Cell diameters were measured directly on the magnified image of the monitor and calculated with a conversion factor (according to the objective magnification).

Cell viability

For CHO cells, this parameter was checked by observing the growth of cells 24 h after pulsing. For leucocytes, Trypan blue penetration (1% w/v) was used to monitor the cell viability 24 h after pulsing.

Experiments were duplicated and deviations are represented as error bars.

The simulation curves were performed with a BASIC program run on an Apple IIe microcomputer (U.S.A.) and written in this laboratory.

Results

Theoretical prediction of size specific electroporation

Square wave electrical pulses induce the formation of transient permeated structures [33]. Electroporation is associated to a structural membrane reorganization when the potential difference reaches a given threshold. The external field modulates the potential difference and can make it larger than this critical threshold. The mechanisms by which electrical fields permeabilize cells are not clearly understood. Nevertheless, it is assumed that these structures result from the transmembrane induced potential difference, ΔV . When the total transmembrane potential reaches a threshold value of -250 mV [34], permeabilization occurs in lipid vesicles.

According to Laplace's equation [35,36], the expression of ΔV is:

$$\Delta V = f \cdot g(\lambda) \cdot r \cdot E \cdot \cos \theta \quad (1)$$

where f is a shape factor, g is a membrane permeability (λ) factor, r is the cell radius, E is the field intensity, and θ is the angle between the electrical field and the normal vector to the membrane.

According to this expression, ΔV is a function of both the field intensity and the cell size. A direct consequence is that larger cells are permeabilized at

lower field intensities than smaller cells. From this theoretical prediction, simulations of permeabilization curves of defined size cell populations were run on a computer in order to determine the behaviour of size-heterogeneous cells submitted to electrical pulses. The program is based on Eqn. 1, which can be written:

$$\Delta V = K \cdot r \cdot E \quad (2)$$

to express the threshold in applied field E .

If cells are assumed to be insulating spheres in a conducting medium, K is equal to 1.5 [35,36]. Nevertheless, because cells are not real dielectrics, K should be considered as an adjustable parameter. Experimental results using a threshold value of ΔV equal to 250 mV are indicative of a value of K about 1. It must be emphasized that, in this program, K is considered as constant whatever the cell type.

The threshold transmembrane potential is set to 250 mV [34] and is independent of both the cell type and the nature of the molecules which would cross the membrane. Then the average sizes (r_i, r_k, \dots) of the populations (i, k, \dots) with the standard deviations are entered. For each field intensity, the computer can calculate the limit value r_j from which the permeabilization appears. If r_i is superior or equal to r_j , the cell is considered as permeabilized whereas if r_i is inferior to r_j , the cell is considered as non permeabilized. The various size distributions of cell populations (i, k, \dots) are taken into account and the relative numbers of permeabilized cells are added for each field intensity. The simulation curves displays the number of permeabilized cells versus the field intensity.

Experimental validation on a model system

These simulations were tested on a mixture of CHO cells and erythrocytes. Experiments were first carried out on this model system because erythrocytes are much smaller than CHO cells and both cell types have a narrow size distribution. The size values we used were obtained from direct videomicroscopy observation of the cell suspension. This gives the histograms shown in Fig. 2. The average size was $13 \mu\text{m}$ ($\pm 1 \mu\text{m}$) for CHO cells and was $7.5 \mu\text{m}$ ($\pm 0.5 \mu\text{m}$) for erythrocytes.

Using Eqn. 2, the simulation profiles predicted a similar shape for permeabilization curves of the two cell types (both populations having a narrow size distribution) but a shift of the erythrocytes permeabilization curve towards higher field intensities, due to their smaller sizes (Fig. 3).

Experiments were operated as follows. Cells were mixed after washing (about 1 CHO cell for 100 erythrocytes) and treated with electric fields of increasing intensity. As shown in Fig. 4 (for ten successive pulses of 100 μs duration), permeabilization of CHO cells was observed at field intensities larger than 700 V/cm

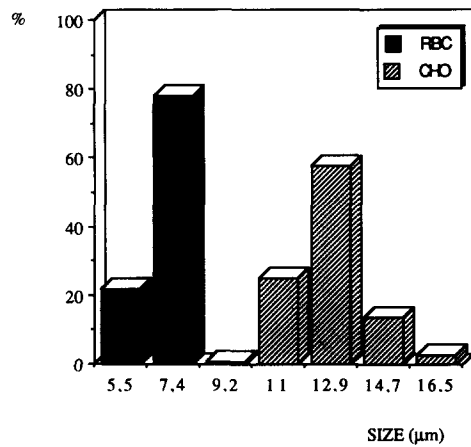


Fig. 2. Size histogram of red blood cells (RBC) and CHO cells.

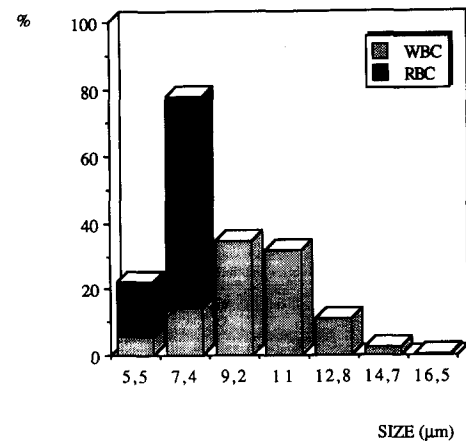


Fig. 5. Size histogram of red blood cells (RBC) and white blood cells (WBC).

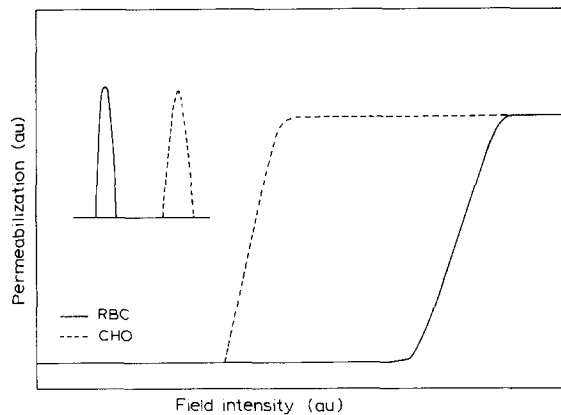


Fig. 3. Simulation of permeabilization curves of red blood cells (RBC) and CHO cells showing predicted numbers of permeabilized cells versus field intensity. This was obtained from the average sizes with the standard deviation of each population ($13 \mu\text{m} \pm 1 \mu\text{m}$ for CHO cells and $7.5 \mu\text{m} \pm 0.5 \mu\text{m}$ for erythrocytes) given in the upper left corner.

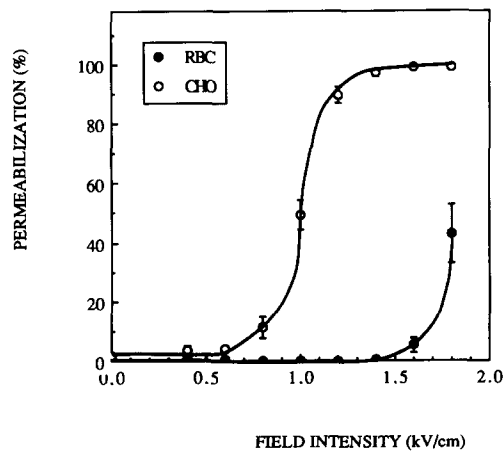


Fig. 4. Batch experiments. Permeabilization curves of CHO cells and red blood cells (RBC) showing the number of permeabilized cells versus field intensity. CHO cell permeabilization was quantitated by counting blue-stained cells while the percentage of haemolysis was the permeabilization indicator for erythrocytes. 100% haemolysis was obtained with erythrocytes lysed in pure water.

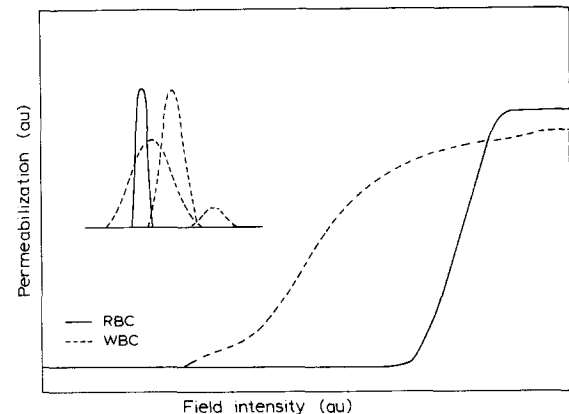


Fig. 6. Simulation of permeabilization curves of red blood cells (RBC) and leucocytes (WBC). The cellular heterogeneity of this population was determined according to experimental data (Fig. 5): small and large lymphocytes ($8.5 \mu\text{m} \pm 3.5 \mu\text{m}$), polymorphs ($11 \mu\text{m} \pm 2 \mu\text{m}$) and monocytes ($16 \mu\text{m} \pm 2 \mu\text{m}$). The average size of erythrocytes was taken as $7.5 \mu\text{m} \pm 0.5 \mu\text{m}$. The size distributions are shown in the upper left corner.

whereas haemolysis of erythrocytes only appeared at a field intensity of 1.6 kV/cm . By applying ten pulses with duration of $100 \mu\text{s}$ between 1.2 and 1.4 kV/cm across this cell suspension, 100% of the CHO were permeabilized, whereas no haemolysis of erythrocytes was detected.

These observations give clear evidence that electro-permeabilization is size-specific in a mixture.

Experimental validation on a blood sample

Blood cells have a much more complicated size distribution and as such are an interesting challenge.

The size histogram of leucocytes (Fig. 5) outlines the cellular heterogeneity of this population: in fact, small and large lymphocytes ($7\text{--}12 \mu\text{m}$), polymorphs ($12\text{--}14 \mu\text{m}$) and monocytes ($15\text{--}20 \mu\text{m}$) are the three subclasses of leucocytes. The experimental size data of leucocytes were fed in the program which can take the three

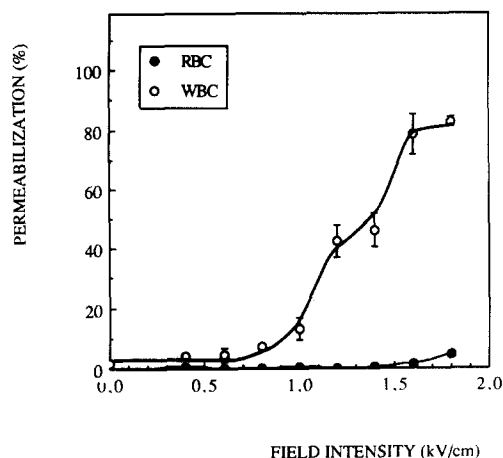


Fig. 7. Batch experiments. Permeabilization curves of white blood cells (WBC) and red blood cells (RBC). Leucocyte permeabilization was quantitated by counting blue-stained cells, while percentage of haemolysis was the permeabilization indicator for erythrocytes. 100% haemolysis was obtained with erythrocytes lysed in pure water.

different populations into account to predict the permeabilization curve. Results are presented in Fig. 6 and show a slow increase of the percentage of permeabilized cells. As described above, the permeation profile of erythrocytes is associated with higher field strengths. Nevertheless, it should be noted that 100% permeabilization is predicted to be obtained with erythrocytes at a lower field than with leucocytes, although the threshold field intensity of erythrocytes is higher than for leucocytes.

Cells were not washed before pulsing to prevent the putative damaging effects of centrifugation. Large molecules were then present in the plasma, i.e., in the pulsing buffer. Results obtained in this laboratory [33] showed that the presence of high-molecular-weight molecules, such as serum albumin from the plasma, would shift the permeabilization curves to higher field intensities.

The experimental results described in Fig. 7 are in agreement with these previous results: permeabilization of erythrocytes appeared only with a field intensity of 1.8 kV/cm. The leucocyte permeabilization curve exhibits a complicated pattern, as predicted in Fig. 6. Indeed, the slope of the curve is small and the whole population cannot be permeabilized by fields smaller than 2 kV/cm, as predicted. The erythrocytes with an average size of 7.5 μm have similar size as for small lymphocytes and a threshold field intensity about 1.6 kV/cm.

Ten pulses applied on blood cells with a duration of 100 μs and a field intensity of 1.6 kV/cm permeabilize 90% of the leucocytes but not erythrocytes. This observation confirms the size specificity of electroporation in a biological fluid.

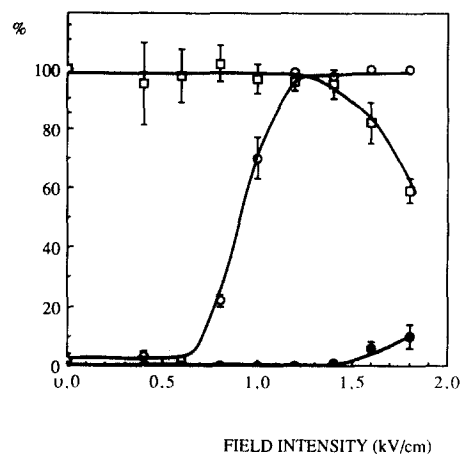


Fig. 8. Continuous flow experiments. Permeabilization curves of CHO cells (○) and erythrocytes (●). CHO cells permeabilization was quantitated by counting blue-stained cells and percentage of haemolysis was the permeabilization indicator for erythrocytes. CHO cell (□) viability was measured after 24 h by the Trypan blue test.

Specific permeabilization of a large volume of cell suspension

In previous batch experiments, 250 μl of cell suspension was put between the electrodes and pulsed (ten pulses with a duration of 100 μs and a frequency of 1 Hz). To increase the number of pulsed cells, this procedure was changed to a flow procedure. As described in 'Materials and Methods', by synchronously pulsing a flow of cells, pulses lasted 100 μs with a frequency of 10 Hz. The flow rate was 11 ml/min, resulting in seven pulses applied for each cell.

As described above, a mixture of CHO cells and erythrocytes in PB was first treated. Results shown in Fig. 8 are indicative that the permeabilization occurs as in the batch experiments (Fig. 4).

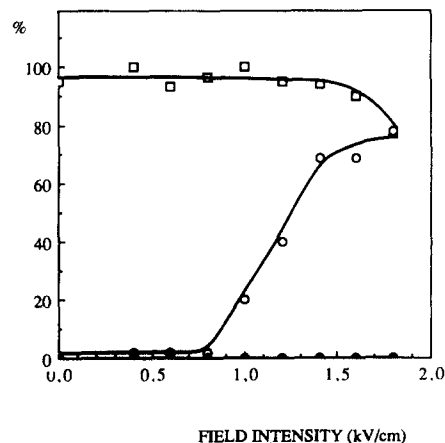


Fig. 9. Continuous flow experiments. Permeabilization curves of leucocytes (○) and erythrocytes (●). Leucocyte permeabilization was quantitated by counting blue-stained cells and percentage of haemolysis was the permeabilization indicator for erythrocytes. Leucocyte viability (□) was measured after 24 h by the Trypan blue test.

It was important to check that the stress due to the flow was not lethal to pulsed cells, so we followed the growth of cells (control and pulsed cells) for 24 h. The results (Fig. 8) show that viability was not affected up to 1.5 kV/cm. Consequently, by applying ten pulses lasting 100 μ s with a field intensity of 1.4 kV/cm, 100% of CHO cells are permeabilized without alteration of their viability and erythrocytes are not haemolysed.

This procedure was extended to a blood sample. Cells were directly pulsed in plasma and permeabilization rates were recorded (Fig. 9). Results obtained with the flow system were similar to those of batch experiments. The shift in the profile is due to our observation that blood samples have various leucocyte size distributions from one patient to another. Leucocyte viability was controlled by the Trypan blue procedure: the viability decreased only above 1.6 kV/cm. Thus, at this field value, 70% of the leucocytes (polymorphs and monocytes) are permeabilized without alteration of viability.

Discussion

Our results show both mathematically and experimentally that the physical basis underlying electroporation is valid on biological systems. Our main observation is that the cell membrane can not be considered as a pure dielectric but rather as a poor conducting system. This conclusion is reached from the necessity to use a value of the parameter K (in Eqn. 1) equal to 1 and not to 1.5. As this value is valid whatever the cell type which is pulsed (erythrocytes, CHO cells, leucocytes), we must conclude that the electrical characteristics of the cell membrane are not strain-dependent. This conclusion shows that the cell diameter is the parameter to be taken into account in the field dependence of electroporation.

As a model system, CHO cells/erythrocytes mixture was used for permeabilization assays. The comparison of the size histogram (Fig. 2) with the permeabilization curves (Fig. 4) agrees with the prediction: CHO cell threshold is about 600 V/cm, whereas erythrocyte threshold is 1.4 kV/cm. The simulation curves are supported by the experimental data showing the size specific permeabilization of cell mixtures.

This property was extended to a physiological system with blood samples. Due to the broad size distribution of leucocytes (Fig. 5), the simulation curve predicts a complex nature of leucocytes permeabilization and the need of a very high field intensity to permeabilize the whole population. It must be noticed that as small lymphocytes have similar or smaller size than erythrocytes, it was predicted by the computer that the curves should cross and this was confirmed by the experimental results.

This size-specific permeabilization was used for electropulsing of large volumes of cells, by using a flow system [30,31] as described in Fig. 1. Experiments both on CHO cells (Fig. 8) and on leucocytes (Fig. 9) showed that there was no decrease of the cell viability for the field intensities we used. For the CHO cell/erythrocyte system, the permeabilization/field profiles were the same in the batch and flow systems.

The erythrocyte/leucocyte permeabilization experiments were run in plasma in order to avoid the washing steps and to test the permeabilization in physiological conditions. The shift of the erythrocyte permeabilization curve towards higher field intensities (Fig. 9) is due to the effect of high-molecular-weight molecules which prevent the exchanges of molecules across the plasma membrane during the permeabilization state [33].

Our conclusions are of major practical importance. We describe, on the one hand, electrical conditions suitable for the specific electroporation of leucocytes in a blood sample and, on the other hand, the permeabilization of large volumes of cells under conditions which do not affect their viability.

Interest concerning the use of permeabilized cells as drug vehicles has up to now been focused on erythrocytes [11] or platelets [26]. In all cases, these applications require isolation of target cells from a blood sample before treating and injecting back the electroloaded cells to the donor. The results presented in this study open up new prospects with the ability to specifically electroporate (or electroload, or electrotransform) leucocytes in blood samples without any isolation step. The flow system can be adapted to an extracorporeal circulation in order to treat the whole blood volume. In this laboratory we are currently studying the possibility of using leucocytes (polymorphs and monocytes) electroloaded with an antibiotic or an anti-inflammatory drug as efficient delivery vehicles to sites of infection.

Acknowledgements

Thanks are due to Mrs J. Zalta, who cared for the CHO cells, to Mr B. Gabriel for his contribution for the stimulation program and to Mr. J. Coveney for rereading the manuscript.

References

- 1 Escande-Géraud, M.L., Rols, M.P., Dupont, M.A., Gas, N. and Teissié, J. (1988) *Biochim. Biophys. Acta* 939, 247-259.
- 2 Mir, L.M., Banoun, H. and Paoletti, C. (1988) *Exp. Cell Res.* 175, 15-25.
- 3 Melvik, J.E., Pettersen, E.O., Gordon, P.B. and Seglen, P.O. (1986) *Eur. J. Cancer Clin. Oncol.* 22, 1523-1530.
- 4 Jastreboff, M.M., Sokolowski, J.A., Bertino, J.R. and Narayanan, R. (1987) *Biochem. Pharmacol.* 36, 1345-1348.

- 5 Orlowski, S., Belehradek, J. Jr., Paoletti, C. and Mir, L.M. (1988) *Biochem. Pharmacol.* 37, 4727–4734.
- 6 Mühlig, P., Förster, W., Jacob, H.E., Berg, H., Röglin, G. and Wohlrabe, K. (1984) *Studia Biophys.* 104, 207–213.
- 7 Neumann, E., Schaeffer-Ridder, M., Wang, Y. and Hofschneider, P.H. (1982) *EMBO J.*, 1, 841–845.
- 8 Baker, P.F. and Knight, D.E. (1983) *Methods Enzymol.* 98, 28–37.
- 9 Zimmermann, U., Riemann, F. and Pilwat, G. (1976) *Biochim. Biophys. Acta* 436, 460–474.
- 10 Kinosita, K. Jr. and Tsong, T.Y. (1977) *Nature* 268, 438–441.
- 11 Kinosita, K. Jr. and Tsong, T.Y. (1978) *Nature* 272, 258–260.
- 12 Jastreboff, M.M., Ito, E., Bertino, J.R. and Narayanan, R. (1987) *Exp. Cell Res.* 171, 513–517.
- 13 Van Brunt, J. (1987) *Biotechnology* 7, 127–130.
- 14 Fiani, M.L. and Stahl, P.D. (1989) *Trends Biotechnol.* 7, 57–61.
- 15 Gabizon, A. and Papahadjopoulos, D. (1988) *Proc. Natl. Acad. Sci. USA* 85, 6949–6953.
- 16 Gregoriadis, G. (1985) *Trends Biotechnol.* 3, 235–241.
- 17 Zimmermann, U. (1983) in *Targeted Drugs* (Goldberg, E.P., ed.), Wiley, New York.
- 18 Lewis, D.A. and Alphar H.O. (1984) *Int. J. Pharm.* 22, 137–146.
- 19 Tomlinson, E. (1987) *Adv. Drug Deliv. Rev.* 187–198.
- 20 Langer, R., Brem, H. and Langer, L.F. (1989) *Neurobiol. Aging* 5, 642–643.
- 21 Aston, R., Holder, A.T., Ivanyi, J. and Bomford, R. (1987) *Mol. Immunol.* 24, 143–150.
- 22 Till, H.A., Ghetie, V., Gregory, T., Patzer, E., Porter, J.P., Uhr, J.W., Capon, D. and Vitetta, E.S. (1988) *Science* 242, 1166–1168.
- 23 Bagshawe, K.D., Springer, C.J., Searle, F., Antonin, P., Sharma, S.K., Melton, R.G. and Sherwood, R.F. (1988) *Br. J. Cancer* 58, 700–703.
- 24 Wilk, S., Mizoguchi, H. and Orlowski, M. (1978) *J. Pharmacol. Exp. Ther.* 206, 227–232.
- 25 Gregoriadis, G. (1977) *Nature* 265, 407–411.
- 26 Hughes, K. and Crawford, N. (1989) *Biochim. Biophys. Acta* 981, 277–287.
- 27 Darnault, P., Bretagne, J.P., Moisan, A., Lecloirec, J., Morisot, D. and Herry, J.Y. (1985) *Gastroenterol. Clin. Biol.* 9, 690–696.
- 28 Potter, H., Weir, L. and Leder, P. (1984) *Proc. Natl. Acad. Sci. USA* 81, 7161–7165.
- 29 Toneguzzo, F., Hayday, A.C. and Keating, A. (1986) *Mol. Cell Biol.* 6, 703–706.
- 30 Teissié, J. and Conté, P. (1988) *Bioelectrochem. Bioenerg.* 19, 49–57.
- 31 Teissié, J. and Rols, M.P. (1988) *Bioelectrochem. Bioenerg.* 19, 49–57.
- 32 Teissié, J. and Rols, M.P. (1988) in 'Dynamics of Membrane Proteins and Cellular Energetics' (Lattruffe, N., Gaudemer, Y., Vignais, P. and Azzi, A., eds.) pp. 115–127, Springer, Berlin.
- 33 Rols, M.P. and Teissié, J. (1989) *Eur. J. Biochem.* 179, 109–115.
- 34 Teissié, J. and Tsong, T.Y. (1981) *Biochemistry* 20, 1548–1554.
- 35 Sale, A.J.H. and Hamilton, W.A. (1968) *Biochim. Biophys. Acta* 163, 37–43.
- 36 Bernhardt, J. and Pauly, H. (1973) *Biophysik* 10, 89–98.